

A *SCN10A* SNP biases human pain sensitivity

Guangyou Duan, MD^{1,2,*}, Chongyang Han, PhD^{3,4,*},
Qingli Wang, MD^{1,5}, Shanna Guo, MD¹, Yuhao Zhang, MD¹,
Ying Ying, MSc¹, Penghao Huang, MSc¹, Li Zhang, MSc¹,
Lawrence Macala, MSc^{3,4}, Palak Shah, MSc^{3,4}, Mi Zhang, MSc¹,
Ningbo Li, MSc¹, Sulayman D Dib-Hajj, PhD^{3,4},
Stephen G Waxman, MD, PhD^{3,4} and Xianwei Zhang, MD¹

Abstract

Background: Nav1.8 sodium channels, encoded by *SCN10A*, are preferentially expressed in nociceptive neurons and play an important role in human pain. Although rare gain-of-function variants in *SCN10A* have been identified in individuals with painful peripheral neuropathies, whether more common variants in *SCN10A* can have an effect at the channel level and at the dorsal root ganglion, neuronal level leading to a pain disorder or an altered normal pain threshold has not been determined.

Results: Candidate single nucleotide polymorphism association approach together with experimental pain testing in human subjects was used to explore possible common *SCN10A* missense variants that might affect human pain sensitivity. We demonstrated an association between rs6795970 (G > A; p.Ala1073Val) and higher thresholds for mechanical pain in a discovery cohort (496 subjects) and confirmed it in a larger replication cohort (1005 female subjects). Functional assessments showed that although the minor allele shifts channel activation by -4.3 mV, a proexcitatory attribute, it accelerates inactivation, an antiexcitatory attribute, with the net effect being reduced repetitive firing of dorsal root ganglion neurons, consistent with lower mechanical pain sensitivity.

Conclusions: At the association and mechanistic levels, the *SCN10A* single nucleotide polymorphism rs6795970 biases human pain sensitivity.

Keywords

Nav1.8, dorsal root ganglion, pain, voltage-gated sodium channel

Date received: 18 May 2016; revised: 11 July 2016; accepted: 19 July 2016

Background

The Nav1.8 sodium channel, encoded by *SCN10A*, is preferentially expressed in dorsal root ganglion (DRG) and trigeminal ganglion neurons, most of which are nociceptive, and is also present along peripheral axon and free nerve terminals in skin and cornea.^{1–4} The biophysical properties of Nav1.8, its critical role in repetitive firing, and its presence in free nerve endings, suggest that Nav1.8 can significantly influence nociceptor excitability, thus contributing to pain.^{5–8} Indeed, relatively rare gain-of-function variants in *SCN10A* have been identified in individuals with painful peripheral neuropathies.^{9–11} However, whether more common variants in *SCN10A* can have an effect at the channel level and at

¹Department of Anesthesiology, Tongji Hospital, Tongji Medical College, Huazhong University of Science and Technology, Wuhan, P.R. China

²Department of Anesthesiology, Xinqiao Hospital, Third Military Medical University, Chongqing, P.R. China

³Department of Neurology and Center for Neuroscience and Regeneration Research, Yale University School of Medicine, New Haven, CT, USA

⁴Rehabilitation Research Center, Veterans' Affairs Connecticut Healthcare System, West Haven, CT, USA

⁵Department of Anesthesiology, Wuhan General Hospital of Guangzhou Military, Wuhan, P.R. China

*Authors Duan G and Han C contributed equally.

Corresponding authors:

Stephen G. Waxman, Center for Neuroscience and Regeneration Research, Veterans' Affairs Connecticut Healthcare System, 950 Campbell Avenue, Building 34, West Haven, CT 06516, USA.

Email: stephen.waxman@yale.edu

Xianwei Zhang, Department of Anesthesiology, Tongji Hospital of Tongji Medical College, Huazhong University of Science and Technology, 1095 Jie Fang Avenue, Wuhan 430030, P.R. China.

Email: ourpain@163.com



Table 1. Comparison of characteristics between male and female undergraduates in discovery study and patient subjects in replication study.

	Male undergraduates (n = 187)	Female undergraduates (n = 309)	Female patient subjects (n = 1005)	ANOVA P
Age (year)	22.8 ± 2.3	22.5 ± 2.2	38.5 ± 10.9*†	P < 0.001
BMI (kg/m ²)	21.8 ± 2.5	19.8 ± 1.9*	22.3 ± 3.4†	P < 0.001
D-PPT (kg/cm ²)	3.86 ± 1.39	2.87 ± 1.00*	2.34 ± 0.97*†	P < 0.001
D-PTO (kg/cm ²)	8.11 ± 2.69	5.33 ± 1.88*	4.65 ± 1.66*†	P < 0.001
S-PPT (kg/cm ²)	17.2 ± 5.3	13.1 ± 3.7*	10.3 ± 4.3*†	P < 0.001
S-PTO (kg/cm ²)	39.2 ± 13.9	26.1 ± 9.5*	18.9 ± 8.3*†	P < 0.001
QPT (kg/cm ²)	54 ± 16	44 ± 14*	26 ± 12*†	P < 0.001
WLT (s)	6.6 ± 3.3	6.2 ± 3.2	Null	P = 0.187

ANOVA: analysis of variance; D-PPT: dull pressure pain threshold; D-PTO: dull pressure pain tolerance; S-PPT: sharp pressure pain threshold; S-PTO: sharp pressure pain tolerance; QPT: quantizing pricking pain; WLT: withdrawal latency time. Compared to male undergraduates, *P < 0.001; compared to female undergraduates, †P < 0.001.

the DRG, neuronal level leading to a pain disorder or an altered normal pain threshold have not been determined.

Interestingly, several genome-wide association studies in diverse ethnic populations have identified associations of single nucleotide polymorphisms (SNPs) in *SCN10A* with cardiac conduction.^{12–21} The SNP rs6795970 (nucleotide level: NM_006514.2: c.3218 G > A) whose minor allele causes a nonsynonymous substitution (NP_006505.2: p.Ala1073Val) and rs12632942 (c.3218A > G, p.Leu 1092 Pro)^{21–24} are the most frequently reported *SCN10A* SNPs that correlate with cardiac conduction.^{12–21} Although the role of these substitutions in cardiac conduction are not well understood,^{13,21–26} these findings provided a good candidate strategy for exploring the common *SCN10A* variant that may affect human pain sensitivity.

Using a targeted SNP approach together with experimental pain testing in human subjects, we explored the possible associations between human pain sensitivity and the previously described common *SCN10A* SNPs, rs6795970 and rs12632942, and additional nonsynonymous SNPs with a minor allele frequency ≥ 5% (dbSNP database, <http://www.ncbi.nlm.nih.gov/snp/>). Electrophysiological recordings in DRG neurons were used to test whether the rs6795970, the SNP that is associated with experimental pain in our study, may alter channel properties and firing properties of DRG neurons. The combination of genotype screening and experimental pain testing in humans and functional testing in DRG neurons demonstrates, at the association and mechanistic levels, that the *SCN10A* SNP may bias human pain sensitivity.

Methods

Association study

Subjects. Subjects were enrolled in our study over the period from August 2013 to December 2014 to explore

associations between pain-related genes and human pain sensitivity in a general population. The cohort in the current study was expanded from our previous study.²⁷ The study protocol was approved by the Institutional Ethics Committee of Tongji Hospital, Tongji Medical College, Huazhong University of Science and Technology. Written informed consent was obtained from all participants prior to the initiation of the study.

In the current study, we included a total of 496 healthy male and female undergraduates of Han Chinese ethnic origin at Huazhong University of Science and Technology for our discovery cohort; demographic data are presented in Table 1. Because of pressure pain threshold asymmetry of left and right handers,²⁸ all enrolled subjects were right-hand dominant. Exclusion criteria included use of any analgesic medication within the four weeks prior to the study, alcohol or drug abuse, pregnancy or lactation, or presence of dermatitis or damaged, red, or swollen skin at the selected testing locations.

Establishing a positive replication of genotype-phenotype correlation requires a more stringent and powerful cohort than the original cohort,²⁹ and population stratification can be a major confounder of data in association studies.³⁰ It was necessary to control for sex in the replication study because we detected significant differences in experimental pain sensitivity between males and females in our discovery study (Table 1). In addition, enrollment of subjects undergoing gynecological surgery in one specific hospital ward could also make recruitment easier and ensured a consistent research environment for the study subjects, and our research group has recently focused on female pain perception.^{27,31,32} Therefore, a total of 1005 Han Chinese women who were scheduled for elective gynecological surgery were included in the replication cohort.

Female subjects in the replication sample were included based on set inclusion and exclusion criteria.

The inclusion criteria were as follows: Han Chinese, right-hand dominant, and scheduling for gynecological surgery. The exclusion criteria were as follows: incapable of communicating, smoking, alcohol, drug abuse, pregnancy or at menstrual period, use of any analgesic medication over the previous four weeks, diabetes mellitus, severe cardiovascular diseases, and kidney or compromised hepatic function. On the day prior to the operation, research staff screened patients on the gynecological wards for inclusion/exclusion criteria, and patients who were invited to enroll in our study received information to minimize their anxiety related to the surgery and to the experimental pain test. Then, the experimental pain tests for all these subjects were performed using a standard procedure as in the primary study.

Experimental pain measurements

In the current study, we applied dull pressure pain measurement, sharp pressure pain measurement, and quantizing pricking pain (QPT) measurement to assess the subjects' mechanical pain sensitivity as described previously.^{33–35} Heat pain sensitivity was analyzed through withdrawal latency time (WLT) for radiating heat stimulus as reported previously.³⁶ Experimental pain measurements including dull, sharp, pricking, and heat pain measurements were applied by four different investigators, respectively, and for all subjects, each type of measurement was tested on all occasions by the same investigator. Testing for D-PPT (dull pressure pain threshold), D-PTO (dull pressure pain tolerance), S-PPT (sharp pressure pain threshold), S-PTO (sharp pressure pain tolerance), and QPT were carried out by female experimenters, thus minimizing the potential effect of the sex of the experimenter on test results for all the female subjects in both cohorts, which represent 87.5% of the total subjects enrolled in this study. Standardized instruction and initial trial runs of mechanical and heat pain measurements were performed at the outset of each testing session to familiarize the participant with the testing procedure. Because the results of the primary study showed that only mechanical pain sensitivity was associated with *SCN10A* SNPs, mechanical pain sensitivity was preferentially tested for the replication cohort.

In this study, a hand-held electronic mechanical algometer was used to test mechanical pain sensitivity. D-PPT and D-PTO were measured using a mechanical algometer with a 1-cm² probe, while S-PPT and S-PTO were measured using a 0.1-cm² probe. Finally, QPT was measured using a mechanical algometer with a 0.01-cm² probe. The investigator applied the algometer to each of three locations on the right forearm in the following sequential manner: (1) location 1 for D-PPT and D-PTO (the lateral brachioradialis of the elbow joint); (2)

location 2 for S-PPT and S-PTO (the midpoint between locations 1 and 3); and (3) location 3 for QPT (the midpoint of the medial and lateral borders of the wrist).

A standardized procedure was used for all participants. Participants were asked to say "pain" when they started to feel pain (D-PPT, S-PPT, or QPT) during the stimulation; the stimulation was restarted after a brief pause following this statement, and the participants were asked to state "okay" when the pain became intolerable (D-PTO or S-PTO). Each pain test was repeated 5 min later, and the average of the two measurements was calculated. The order of the pain tests was identical for all subjects.

WLT was measured using an Ugo Basile Biological Apparatus (model 37370; Ugo Basile, Italy), with infrared radiance intensity set at 60. The participants positioned their middle finger above the infrared generator. The investigator then activated both the infrared source and a reaction time counter via a start key. Participants were told to withdraw their finger when they started to feel pain; at this point, the infrared beam was automatically switched off, and the timer stopped. The left and right middle fingers of each participant were measured, and the average WLT of the two measurements was calculated.

Genotyping

Heparin-treated blood was collected for all subjects from the antecubital vein. Genomic DNA was extracted from blood samples using the guanidinium isothiocyanate method. Genotyping of *SCN10A* SNPs was performed by Shanghai BioWing Applied Biotechnology Company (<http://www.biowing.com.cn/>) using ligase detection reactions (LDRs).³⁷ The target DNA sequences were amplified using a multiplex PCR method. After completion of the amplification, the ligation reaction for each subject was carried out and LDR was performed using 40 cycles of 94°C for 30 s and 63°C for 4 min. The fluorescent products of LDR were differentiated using an ABI sequencer 377. In addition to the rs6795970 and rs12632942, three SNPs, i.e. rs57326399 (c.2884A > G, Ile962Val), rs7630989 (c.1525T > C, Ser509Pro), rs74717885 (c.618 A > G, Ile206Met), were selected based on their locations in exons, their predicted amino acid substitutions, and a minor allele frequency $\geq 5\%$. A total of five *SCN10A* SNPs were screened in the discovery study (Figure 1). Based on the results of the association analysis in the discovery cohort, only rs6795970 and rs12632942 were screened in the replication study.

Statistical analysis

The sample was tested for each SNP to determine whether the null hypothesis of the Hardy-Weinberg

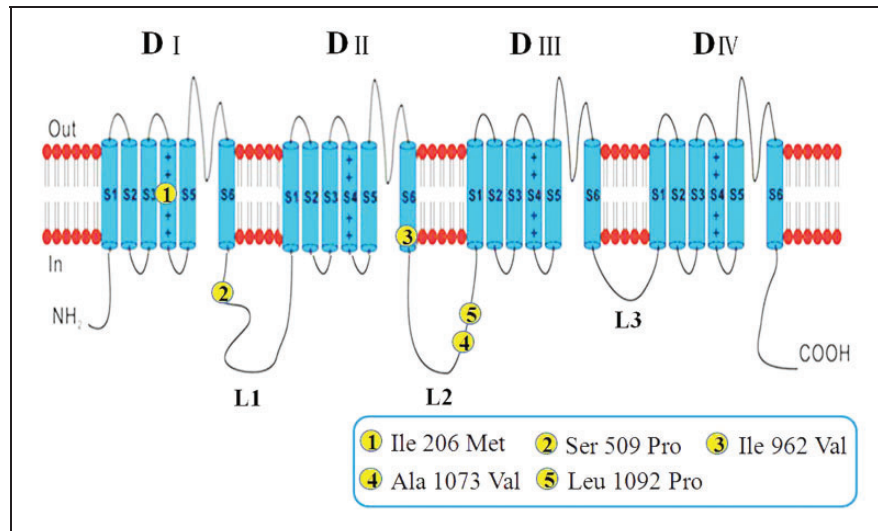


Figure 1. Schematic of sodium channel polypeptide showing the locations of the corresponded amino acid residues encoded by the five *SCN10A* SNPs.

equilibrium (HWE) could be rejected by applying the chi-square method. In both the discovery and replication cohorts, demographic analysis, independent-sample *t* test, and one-way analysis of variance (ANOVA) test of quantitative traits were conducted using the SPSS Statistics Version 17.0 statistical package (SPSS Statistics, Inc., Chicago, IL). In order to reduce the incidence of false negatives in our exploration of the possible association of *SCN10A* SNPs with experimental pain sensitivity in the discovery study, the post hoc least-significant difference (LSD) test was used instead of correction for ANOVA repeated measure analysis for multiple comparisons. We applied Bonferroni (BONF) correction to control for the ANOVA test for replication study, and the *P* values were further multiplied by 10, to correct for the number of tested phenotypes (five) and screened SNPs (two). Post hoc BONF correction test was used for multiple comparisons in the replication study. All analyses used the maximum number of cases available for each experimental pain phenotype. A two-tailed probability value of $P < 0.05$ was used as the criterion for statistical significance.

Functional assessments of Nav1.8 variants

Plasmids. The *pcDNA5-SCN10A* (Nav1.8-Val1073) plasmid construct was purchased from Genionics. Using Mega mutagenesis protocol, a sequence encoding enhanced green fluorescent protein was cloned upstream of the Nav1.8 ATG with a “stopGo” 33 amino acid 2A linker, such that the GFP-2A adaptor and the Nav1.8 channel proteins were produced as independent proteins from the same messenger RNA.^{38–40} Pilot experiments confirmed the presence of GFP-2A and Nav1.8 channels

as independent proteins on Western blots and demonstrated that the channel produces the expected TTX-resistant slowly inactivating current. The nucleotide substitution c.3218A > G which leads to the amino acid substitution Val1073Ala was introduced into the construct using QuikChange® II XL site-directed mutagenesis (Stratagene). Each batch of the plasmids that were used in this study were verified by Sanger sequencing and confirmed to produce the Nav1.8 current in a heterologous expression system before using it in the experiments.

Primary mouse DRG neuron isolation and transfection. Animal studies were approved by Veterans Administration West Haven medical center Animal Use Committees. DRG neurons were isolated, as previously reported,⁴¹ from homozygous Nav1.8-cre mice (four–eight weeks of age, both male and female) that lack endogenous Nav1.8.^{9,10,42} In compliance with the recent NIH guidelines and our own practice, we have used both male and female mice as source for DRG neurons. DRG cultures for voltage-clamp analysis were made from six mice each (three male and three female) for the Ala1073 and the Val1073 recordings; and for current-clamp analysis, we used six mice (four female and two male) for the Ala1073 and seven mice (four female and three male) for the Val1073 analysis. Briefly, DRGs were harvested, incubated at 37°C for 20 min in complete saline solution (in mM: 137 NaCl, 5.3 KCl, 1 MgCl₂, 25 sorbitol, 3 CaCl₂, and 10 N-2-hydroxyethylpiperazine-N’-2-ethanesulfonic acid (HEPES), adjusted to pH 7.2 with NaOH) containing 0.5 U/ml Liberase TM (Roche Diagnostics) and 0.6 mM EDTA before 15 min incubation at 37°C in complete saline solution containing 0.5 U/ml Liberase TL

(Roche Diagnostics), 0.6 mM EDTA, and 30 U/ml papain (Worthington). Tissue was then centrifuged and triturated in 0.5 ml of DRG media: Dulbecco's Modified Eagle Medium/F12 (1:1) with 100 U/ml penicillin, 0.1 mg/ml streptomycin (Invitrogen), and 10% fetal bovine serum (Hyclone), containing 1.5 mg/ml bovine serum albumin (low endotoxin; Sigma), and 1.5 mg/ml trypsin inhibitor (Sigma). After trituration, Nav1.8-Val1073 or Nav1.8-Ala1073 channel constructs were transfected into DRG neurons in suspension using a Nucleofector IIS electroporator (Lonza) and Amaxa SCN Nucleofector reagents (VSP1-1003). After electroporation, 100 μ l of calcium-free Dulbecco's modified Eagle medium (Invitrogen) was added, and cells were incubated at 37°C for 5 min in a 95% air/5% CO₂ (vol/vol) incubator to allow neurons to recover. The cell mixture was then diluted with DRG media containing 1.5 mg/ml bovine serum albumin (low endotoxin; Sigma) and 1.5 mg/ml trypsin inhibitor (Sigma), seeded onto poly-D-lysine/laminin-coated coverslips (BD Bioscience), and incubated at 37°C to allow DRG neurons to attach to the coverslips. After 40 min, DRG media was added into each well to a final volume of 1.0 ml (for current-clamp recording culture, medium was supplemented with 50 ng/ml mouse nerve growth factor (mNGF) (Alomone Labs) and 50 ng/ml recombinant human glial cell line-derived neurotrophic factor (hGDNF) (PeproTech)) and the DRG neurons were maintained at 37°C in a 95% air/5% (vol/vol) CO₂ incubator for 40~48 h before recording.

Electrophysiology

Voltage-clamp recording from transfected mouse DRG neurons. Voltage-clamp recordings were performed with an EPC-10 amplifier (HEKA) from small transfected mouse DRG neurons (<25- μ m diameter) with robust green fluorescence and no apparent neurites at room temperature (~22°C) 40–48 h after transfection as described previously.^{9–11} Fire-polished electrodes (1–2 M Ω) were fabricated from 1.6 mm outer diameter borosilicate glass micropipettes (World Precision Instruments, Sarasota, FL). The pipette potential was adjusted to zero before seal formation, and liquid junction potential was not corrected. Capacitive transients were cancelled, and voltage errors were minimized with 80%–90% series resistance compensation; cells were excluded from analysis if the predicted voltage error exceeded 4 mV. Currents were acquired with PatchMaster software (HEKA Electronics), 5 min after establishing whole-cell configuration, sampled at a rate of 50 kHz, and filtered at 2.9 kHz. The pipette solution contained the following (in mM): 140 CsF, 10 NaCl, 1 EGTA, and 10 HEPES, pH 7.3 with CsOH (adjusted to 315 mOsmol/L with dextrose). The extracellular bath

solution contained the following (in mM): 70 NaCl, 70 choline chloride, 3 KCl, 1 MgCl₂, 1 CaCl₂, 10 HEPES, 5 CsCl, 20 tetraethylammonium chloride (TEA·Cl), pH 7.32 with NaOH (327 mOsmol/L). TTX (0.5 μ M), CdCl₂ (0.1 mM), and 4-aminopyridine (1 mM) were added in the bath solution to block endogenous voltage-gated sodium currents, calcium currents, and potassium currents, respectively.

For current–voltage relationships, cells were held at –70 mV and stepped to a range of potentials (–70 to +40 mV in 5 mV increments) for 100 ms. Peak inward currents (I) were plotted as a function of depolarization potential to generate I – V curves. Activation curves were obtained by converting I to conductance (G) at each voltage (V) using the equation $G = I / (V - V_{rev})$, where V_{rev} is the reversal potential which was determined for each cell individually. Activation curves were then fit with Boltzmann functions in the form of $G = G_{max} / \{1 + \exp[(V_{1/2,act} - V) / k]\}$, where G_{max} is the maximal sodium conductance, $V_{1/2,act}$ is the potential at which activation is half-maximal, V is the test potential, and k is the slope factor.

Steady-state fast inactivation was achieved with a series of 500 ms prepulses (–90 to +10 mV in 5 mV increments) and the remaining noninactivated channels were activated by a 40-ms step depolarization to 0 mV. The protocol for slow inactivation consisted of a 30-s step to potentials varying from –120 to 20 mV, followed by a 30-ms step to –70 mV to remove fast inactivation, and a 20-ms step to 0 mV to elicit a test response. Peak inward currents obtained from steady-state fast inactivation and slow inactivation protocols were normalized by the maximum current amplitude and fit with a Boltzmann equation of the form $I / I_{max} = A + (1 - A) / \{1 + \exp[(V - V_{1/2,inact}) / k]\}$, where V represents the inactivating prepulse potential and $V_{1/2,inact}$ represents the midpoint of the inactivation.

Persistent currents were measured as mean amplitudes of currents recorded between 90 and 95 ms after the onset of depolarization and are presented as a percentage of the maximal transient peak current. Ramp currents were elicited with slow ramp depolarization over a 600-ms period at 0.2 mV/ms. The amplitude of ramp current was presented as a percentage of the maximal peak current.

Recovery from fast inactivation was examined using a two-pulse protocol with interpulse intervals varying from 1 to 1025 ms. Recovery rates were measured by normalizing peak current elicited by the test pulse (10-ms depolarization to 0 mV) to that of the prepulse (100 ms at 0 mV) after various recovery durations (1–1025 ms) at different recovery potentials. Recovery time constants were calculated using monoexponential fits of the recovery fraction over recovery period.

Current-clamp recording on transfected mouse DRG neurons. Current-clamp recordings were obtained at

room temperature ($\sim 22^{\circ}\text{C}$) using an EPC-10 amplifier (HEKA) from small ($<25\text{-}\mu\text{m}$ diameter) GFP-labeled DRG neurons 40–48 h after transfection as described previously.^{9–11} In order to reduce the observation bias from experimental systems, current-clamp recordings were performed in a blind way. Electrodes had a resistance of 1–3 M Ω when filled with the pipette solution, which contained the following (in mM): 140 KCl, 0.5 EGTA, 5 HEPES, and 3 Mg-ATP, pH 7.3 with KOH (adjusted to 315 mosM with dextrose). The extracellular solution contained the following (in mM): 140 NaCl, 3 KCl, 2 MgCl₂, 2 CaCl₂, and 10 HEPES, pH 7.3 with NaOH (adjusted to 320 mosM with dextrose). Whole cell configuration was obtained in voltage-clamp mode before proceeding to the current-clamp recording mode. Current threshold was determined by the first action potential elicited by a series of 200-ms depolarizing current injections that increased in 5-pA increments. Voltage threshold was determined by assessing the first-order derivative dV/dt of membrane potential. Cells with stable resting membrane potentials more negative than -40 mV and overshooting action potentials (>80 mV resting membrane potential to peak) were used for additional data collection. Action potential frequency was determined by quantifying the number of action potentials elicited in response to depolarizing current injections (500 ms). Membrane potential oscillations were analyzed as previously described^{43,44} and a Fast Fourier Transform (Origin Pro8.5, Origin Lab

Corporation) was used to obtain the frequency components of the oscillations.

Data analysis

Voltage-clamp and current-clamp data were analyzed using FitMaster (HEKA) and OriginPro8.5 (OriginLab Corporation). All data were presented as means \pm SEM. Statistical significance was examined using two-sample Student *t* test, *Scheirer-Ray-Hare* test, or two-portion *z* test.

Results

Association of *SCN10A* SNPs with experimental pain sensitivity: Discovery cohort

Success rates for genotyping the five different *SCN10A* SNPs in the discovery cohort were: rs6795970, 99.8% (495/496); rs12632942, 99.3% (493/496); rs74717885, 100% (496/496); rs7630989, 100% (496/496); and rs57326399, 98.4% (488/496). Data analysis from this discovery cohort showed significant association of rs6795970 (Table 2) with the subjects' mechanical pain sensitivity. However, no significant difference was observed for WLT among subjects carrying the different rs6795970 alleles. The discovery cohort was divided into three groups based upon the composition of the rs6795970 alleles: 359 subjects were homozygous for the major allele G/G (p.Ala1073), 125 subjects were

Table 2. Characteristics of subjects with different *SCN10A* rs6795970 alleles: primary study.

	G/G (n = 359)	G/A (n = 125)	A/A (n = 11)	Statistics
Sex (M / F)	134/225 ($P_1 = 0.076$)	46/79 ($P_2 = 0.080$)	7/4	$\chi^2 = 3.21$; $P = 0.201$
Age (years)	22.6 ± 2.2 ($P_1 = 0.586$)	22.5 ± 2.1 ($P_2 = 0.506$)	23.0 ± 2.3	$F = 0.25$; $P = 0.777$
BMI (kg/m ²)	20.5 ± 2.3 ($P_1 = 0.369$)	20.5 ± 2.6 ($P_2 = 0.348$)	21.2 ± 2.5	$F = 0.44$; $P = 0.643$
D-PPT (kg/cm²)	3.21 ± 1.27 ($P_1 = 0.030$)	3.25 ± 1.23 ($P_2 = 0.044$)	4.04 ± 1.01	$F = 2.36$; $P = 0.095$
D-PTO(kg/cm²)	6.33 ± 2.58 ($P_1 = 0.029$)	6.36 ± 2.54 ($P_2 = 0.036$)	8.05 ± 1.81	$F = 2.41$; $P = 0.091$
S-PPT (kg/cm ²)	14.5 ± 4.4 ($P_1 = 0.409$)	14.8 ± 5.8 ($P_2 = 0.547$)	15.7 ± 5.5	$F = 0.49$; $P = 0.614$
S-PTO (kg/cm ²)	30.9 ± 12.9 ($P_1 = 0.061$)	30.8 ± 13.3 ($P_2 = 0.064$)	38.4 ± 12.5	$F = 1.80$; $P = 0.167$
QPT (kg/cm ²)	48 ± 16 ($P_1 = 0.223$)	46 ± 14 ($P_2 = 0.102$)	54 ± 19	$F = 1.84$; $P = 0.160$
WLT (s)	6.1 ± 3.0 ($P_1 = 0.728$)	6.8 ± 4.0 ($P_2 = 0.288$)	6.2 ± 2.2	$F = 2.13$; $P = 0.119$

BMI: body mass index; D-PPT: dull pressure pain threshold; D-PTO: dull pressure pain tolerance; S-PPT: sharp pressure pain threshold; S-PTO: sharp pressure pain tolerance; QPT: quantizing pricking pain; WLT: withdrawal latency time; P_1 : significance of difference between G/G and A/A; P_2 : between G/A and A/A.

The rows given in bold represents that significant difference ($P < 0.05$) between groups observed.

Table 3. Characteristics of subjects with different *SCN10A* rs12632942 alleles: primary study.

	A/A (n = 166)	A/G (n = 242)	G/G (n = 85)	Statistics
Sex (M /F)	70/96	86/156 ($P_1 = 0.176$)	30/55 ($P_2 = 0.292$)	$\chi^2 = 2.10$; $P = 0.350$
Age (years)	22.6 ± 2.1	22.5 ± 2.3 ($P_1 = 0.519$)	23.1 ± 2.1 ($P_2 = 0.113$)	$F = 2.42$; $P = 0.090$
BMI (kg/m ²)	20.8 ± 2.7	20.3 ± 2.2 ($P_1 = 0.034$)	20.6 ± 2.4 ($P_2 = 0.493$)	$F = 2.29$; $P = 0.102$
D-PPT (kg/cm²)	3.43 ± 1.35	3.18 ± 1.21 ($P_1 = 0.042$)	3.06 ± 1.06 ($P_2 = 0.027$)	$F = 3.14$; $P = 0.044$
D-PTO (kg/cm²)	6.97 ± 2.83	6.09 ± 2.34 ($P_1 = 0.001$)	6.04 ± 2.47 ($P_2 = 0.006$)	$F = 6.90$; $P = 0.001$
S-PPT (kg/cm ²)	15.0 ± 5.5	14.2 ± 4.3 ($P_1 = 0.086$)	14.9 ± 4.7 ($P_2 = 0.816$)	$F = 1.66$; $P = 0.191$
S-PTO (kg/cm ²)	32.7 ± 14.0	30.5 ± 12.6 ($P_1 = 0.093$)	29.0 ± 12.0 ($P_2 = 0.031$)	$F = 2.66$; $P = 0.071$
QPT (kg/cm ²)	49 ± 18	47 ± 14 ($P_1 = 0.355$)	46 ± 14 ($P_2 = 0.164$)	$F = 1.03$; $P = 0.358$
WLT (s)	6.1 ± 3.3	6.5 ± 3.5 ($P_1 = 0.927$)	6.2 ± 2.7 ($P_2 = 0.291$)	$F = 0.65$; $P = 0.523$

BMI: body mass index; D-PPT: dull pressure pain threshold; D-PTO: dull pressure pain tolerance; S-PPT: sharp pressure pain threshold; S-PTO: sharp pressure pain tolerance; QPT: quantizing pricking pain; WLT: withdrawal latency time; P_1 : significance of difference between A/G and A/A; P_2 : between G/G and A/A. Hardy-Weinberg equilibrium (HWE) $P = 0.842$.

The rows given in bold represents that significant difference ($P < 0.05$) between groups observed.

heterozygous for alleles G/A, and 11 subjects were homozygous for the minor allele A/A (p.Val1073). The HWE value of rs6795970 for the discovery cohort was $P = 0.975$, indicating that this population conforms to the genetic equilibrium stipulations. As shown in Table 2, the subjects who carried the minor homozygote allele showed higher D-PPT and D-PTO ($LSD P < 0.05$) than those who carried major homozygote or heterozygote alleles. There was no significant difference in the pain sensitivity of individuals carrying the major homozygote versus heterozygote alleles ($LSD P > 0.05$).

Similar to the results from the analysis of rs6795970, the discovery cohort showed a significant association of rs12632942 with the subjects' mechanical pain sensitivity but not with WLT (Table 3). In the association analysis, no significant difference of experimental pain sensitivity was found in the different genotypes of rs74717885, rs7630989, and rs57326399.

Association of minor allele of rs6795970 with mechanical pain: Replication cohort

Based on the findings from the discovery cohort, we investigated the association of rs6795970 and rs12632942 with mechanical pain sensitivity in a larger replication cohort (1005 subjects). Success rates for genotyping rs6795970 and rs12632942 in the replication cohort were 98.6% and 98.2%, respectively. Data analysis showed a significant association of the rs6795970

alleles with mechanical pain sensitivity as we had found in the discovery cohort. In the replication cohort, 663 subjects were homozygous for the major allele G/G, 297 subjects were heterozygous G/A, and 31 subjects were homozygous for the minor allele A/A. The HWE value for the rs6795970 in this cohort was $P = 0.746$. The data showed that rs6795970 was significantly associated with three types of mechanical pain measures, as was observed in the discovery cohort (Table 4). Figure 2 shows that the mean mechanical pain thresholds in carriers of the minor homozygote allele were higher than those in carriers of the other genotypes, indicating that minor allele of rs6795970 is associated with a decrease in human mechanical pain sensitivity. The significance values (after BONF correction) for the differences of S-PPT (Figure 2(b)) between carriers of the minor homozygote alleles and those with the two other genotypes in the replication cohort reached $(2.3-2.4) \times 10^{-5}$, and the ANOVA statistical test was significant at 3.1×10^{-4} . By contrast, the difference of mechanical pain sensitivity between different genotypes of rs12632942 failed to replicate in all mechanical pain measures (Table 5).

Functional assessments of Nav1.8-Ala1073 and Nav1.8-Val1073 channels in DRG neurons

Our results imply that the p.Ala1073Val substitution in Nav1.8, which corresponds to the minor "A" allele of rs6795970, contributes to reduced mechanical pain

Table 4. Characteristics of patients with different *SCN10A* rs6795970 alleles: replication study.

	G/G (n = 663)	G/A (n = 297)	A/A (n = 31)	Naive <i>P</i> value	BONF <i>P</i> value
Age (years)	38.3 ± 11.0 (<i>P</i> ₁ = 0.740)	38.7 ± 10.9 (<i>P</i> ₂ = 1.000)	40.6 ± 11.2	<i>P</i> = 0.474	NA
BMI (kg/m ²)	22.3 ± 3.4 (<i>P</i> ₁ = 0.553)	22.1 ± 3.3 (<i>P</i> ₂ = 0.337)	23.1 ± 3.4	<i>P</i> = 0.260	NA
D-PPT (kg/cm²)	2.32 ± 0.96 (<i>P</i> = 7.2 × 10⁻⁴)	2.29 ± 0.95 (<i>P</i> = 5.1 × 10⁻⁴)	2.98 ± 1.29	<i>P</i> = 7.5 × 10 ⁻⁴	<i>P</i> = 0.008
D-PTO (kg/cm ²)	4.61 ± 1.68 (<i>P</i> ₁ = 0.121)	4.65 ± 1.65 (<i>P</i> ₂ = 0.074)	5.30 ± 1.38	<i>P</i> = 0.079	<i>P</i> = 0.79
S-PPT (kg/cm²)	10.2 ± 4.1 (<i>P</i> = 2.4 × 10⁻⁵)	10.1 ± 4.5 (<i>P</i> = 2.3 × 10⁻⁵)	13.7 ± 6.9	<i>P</i> = 3.1 × 10 ⁻⁵	<i>P</i> = 3.1 × 10 ⁻⁴
S-PTO (kg/cm²)	18.8 ± 8.2 (<i>P</i> = 0.009)	18.8 ± 8.4 (<i>P</i> = 0.011)	23.3 ± 9.2	<i>P</i> = 0.011	<i>P</i> = 0.11
QPT (kg/cm ²)	27 ± 12 (<i>P</i> ₁ = 0.291)	26 ± 13 (<i>P</i> ₂ = 0.114)	31 ± 11	<i>P</i> = 0.088	<i>P</i> = 0.88

BMI: body mass index; D-PPT: dull pressure pain threshold; D-PTO: dull pressure pain tolerance; S-PPT: sharp pressure pain threshold; S-PTO: sharp pressure pain tolerance; QPT: quantizing pricking pain; NA: not applicable; BONF: Bonferroni; *P*₁: Bonferroni significance of difference between G/G and A/A; *P*₂: between G/A and A/A.

The rows given in bold represents that significant difference (*P* < 0.05) between groups observed.

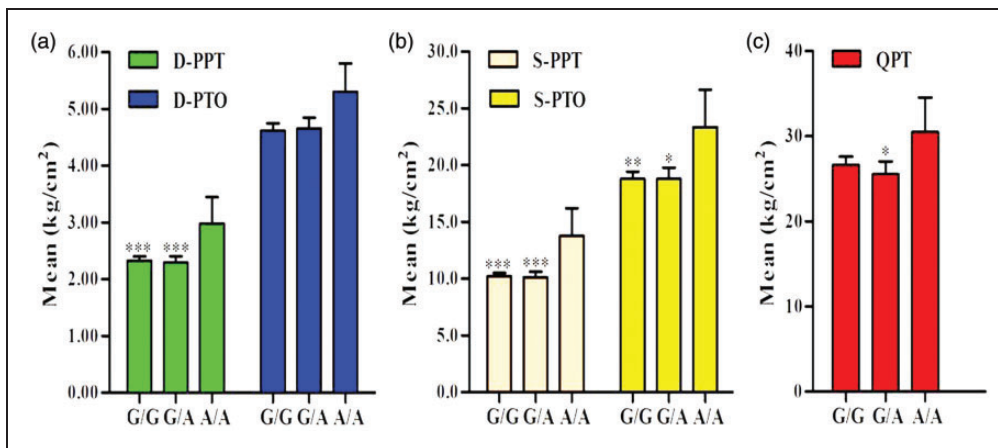


Figure 2. Mean mechanical pain measurement values for the different genotypes of rs6795970 in replication study. (a) dull pressure pain threshold (D-PPT) and dull pressure pain tolerance (D-PTO); (b) sharp pressure pain threshold (S-PPT) and sharp pressure pain tolerance (S-PTO); (c) quantizing pricking pain (QPT). Compared to A/A, *Bonferroni significance of difference *P* < 0.05; ***P* < 0.01; ****P* < 0.001.

sensitivity. To directly examine the effects of this amino acid substitution on the function of Nav1.8 channels and on the excitability of DRG neurons, we transfected either Nav1.8-Ala1073 or Nav1.8-Val1073 channels into Nav1.8 knockout DRG neurons (which lack endogenous Nav1.8) and performed voltage- and current-clamp analyses.

Voltage-clamp analysis

We used voltage-clamp recordings to evaluate the effect of the Ala or Val at position 1073 on the gating properties of Nav1.8. Figure 3 shows representative sodium

channel current traces recorded from DRG neurons transfected with Nav1.8-Ala1073 (Figure 3(a)) and Nav1.8-Val1073 channels (Figure 3(b)). The current density of Nav1.8-Val1073 channels was not significantly different from that of Nav1.8-Ala1073 channels (Nav1.8-Ala1073: 277 ± 41 pA/pF, n = 28; Nav1.8-Val1073: 318 ± 50 pA/pF, n = 20, *P* > 0.05). Nav1.8-Val1073 channels display hyperpolarized activation compared with Nav1.8-Ala1073 channels (Figure 3(c)). The *V*_{1/2} of activation for Nav1.8-Val1073 was -10.9 ± 1.5 mV (n = 20), which represents a 4.3 mV hyperpolarizing shift compared with the *V*_{1/2} of activation for Nav1.8-Ala1073 (-6.6 ± 1.1 mV, n = 28, *P* < 0.05)

Table 5. Characteristics of patients with different *SCN10A* rs12632942 alleles in replication study.

	A/A (n = 421)	A/G (n = 428)	G/G (n = 138)	Naive P value	BONF P value
Age (years)	38.2 ± 11.0	38.6 ± 10.9 ($P_1 = 1.000$)	38.7 ± 11.0 ($P_2 = 1.000$)	$P = 0.850$	NA
BMI (kg/m ²)	22.3 ± 3.5	22.4 ± 3.3 ($P_1 = 1.000$)	22.1 ± 3.4 ($P_2 = 1.000$)	$P = 0.706$	NA
D-PPT (kg/cm ²)	2.37 ± 1.03	2.28 ± 0.91 ($P_1 = 0.444$)	2.41 ± 0.97 ($P_2 = 1.000$)	$P = 0.235$	$P = 1.000$
D-PTO (kg/cm ²)	4.55 ± 1.58	4.71 ± 1.69 ($P_1 = 0.440$)	4.76 ± 1.85 ($P_2 = 1.000$)	$P = 0.282$	$P = 1.000$
S-PPT (kg/cm ²)	10.4 ± 4.6	9.9 ± 4.0 ($P_1 = 0.147$)	10.8 ± 4.3 ($P_2 = 0.418$)	$P = 0.129$	$P = 1.000$
S-PTO (kg/cm ²)	18.4 ± 7.9	19.4 ± 8.8 ($P_1 = 0.221$)	19.2 ± 8.0 ($P_2 = 0.975$)	$P = 0.188$	$P = 1.000$
QPT (kg/cm ²)	26 ± 12	26 ± 13 ($P_1 = 1.000$)	28 ± 13 ($P_2 = 0.152$)	$P = 0.137$	$P = 1.000$

BMI: body mass index; D-PPT: dull pressure pain threshold; D-PTO: dull pressure pain tolerance; S-PPT: sharp pressure pain threshold; S-PTO: sharp pressure pain tolerance; QPT: quantizing pricking pain; NA: not applicable; BONF: Bonferroni; P_1 : Bonferroni significance of difference between A/G and A/A; P_2 : between G/G and A/A. Hardy-Weinberg equilibrium (HWE) $P = 0.084$.

(Figure 3(c)). Figure 3(d) shows that there was no significant difference for the $V_{1/2}$ of fast inactivation between Nav1.8-Val1073 channels (-33.7 ± 1.2 mV, $n = 19$) and Nav1.8-Ala1073 channels (-31.8 ± 0.9 mV, $n = 27$). The $V_{1/2}$ of slow inactivation for Nav1.8-Val1073 was -46.4 ± 1.9 mV ($n = 6$), which was not significant from that of Nav1.8-Ala1073 (-46.3 ± 2.9 mV, $n = 6$, $P > 0.05$) (Figure 3(e)).

The kinetics for open-state inactivation, which reflect the transition from the open to the inactivated state, were significantly faster for Nav1.8-Val1073 channel compared to Nav1.8-Ala1073 channel from -15 to $+15$ mV (Figure 3(f)). We also measured the response to a slow ramp stimulus (-70 to $+50$ mV over 600 ms). The ramp current for Nav1.8-Ala1073 channels ($19.7\% \pm 1.8\%$, $n = 8$) was not significantly different from that of Nav1.8-Val1073 channels ($17.4\% \pm 1.2\%$, $n = 7$). Figure 3(g) compares the normalized amplitudes of persistent current in DRG neurons expressing Nav1.8-Ala1073 and Nav1.8-Val1073 channels. The peak persistent current ($13.5\% \pm 0.7\%$, $n = 20$) for Nav1.8-Val1073 channels was reduced compared to that for Nav1.8-Ala1073 channels ($15.5\% \pm 1.0\%$, $n = 28$); however, this difference did not reach statistical significance. The voltages at which the peak persistent currents occur were -5 mV (Nav1.8-Val1073) and 0 mV (Nav1.8-Ala1073), respectively, consistent with the hyperpolarizing shift in $V_{1/2}$ of activation of the Nav1.8-Val1073 channels (Figure 3(c)).

Recovery from fast inactivation of Nav1.8 channels was investigated at two different physiologically relevant recovery potentials, -50 mV and -70 mV. Compared with Nav1.8-Ala1073 channels, Nav1.8-Val1073

channels tended to show slower recovery from fast-inactivation at -50 mV: the recovery time constants were 13.5 ± 1.6 ms (Nav1.8-Val1073, $n = 5$) and 10.8 ± 1.0 ms (Nav1.8-Ala1073, $n = 10$). The recovery time constants at -70 mV also tended to be slower for Nav1.8-Val1073 channels (4.3 ± 0.5 ms, $n = 6$) compared to Nav1.8-Ala1073 channels (3.3 ± 0.3 ms, $n = 10$). Although Nav1.8-Val1073 channels displayed slower recovery from inactivation compared to Nav1.8-Ala1073 channels (Figure 3(h)), the difference did not reach statistical significance ($P > 0.05$).

Current-clamp analysis

In order to compare the effects of the two channel variants on the excitability of DRG neurons, we carried out current-clamp analysis on DRG neurons transfected with either Nav1.8-Ala1073 or Nav1.8-Val1073 channels. The resting membrane potential of DRG neurons expressing the Nav1.8-Val1073 channels (-57.8 ± 1.3 mV, $n = 33$) was comparable to that DRG neurons expressing Nav1.8-Ala1073 channels (-57.6 ± 1.1 mV, $n = 29$, $P > 0.05$). The input resistance of DRG neurons expressing Nav1.8-Val1073 channels (363 ± 35 M Ω , $n = 33$) was also comparable to that of DRG neurons expressing Nav1.8-Ala1073 channels (364 ± 46 M Ω , $n = 29$, $P > 0.05$). Current thresholds for generation of the first all-or-none action potential were not significantly different between the group of DRG neurons expressing Nav1.8-Val1073 channels (115 ± 11 pA, $n = 33$) and the group of DRG neurons expressing Nav1.8-Ala1073 channels (120 ± 17 pA, $n = 29$, $P > 0.05$). We also compared the voltage threshold

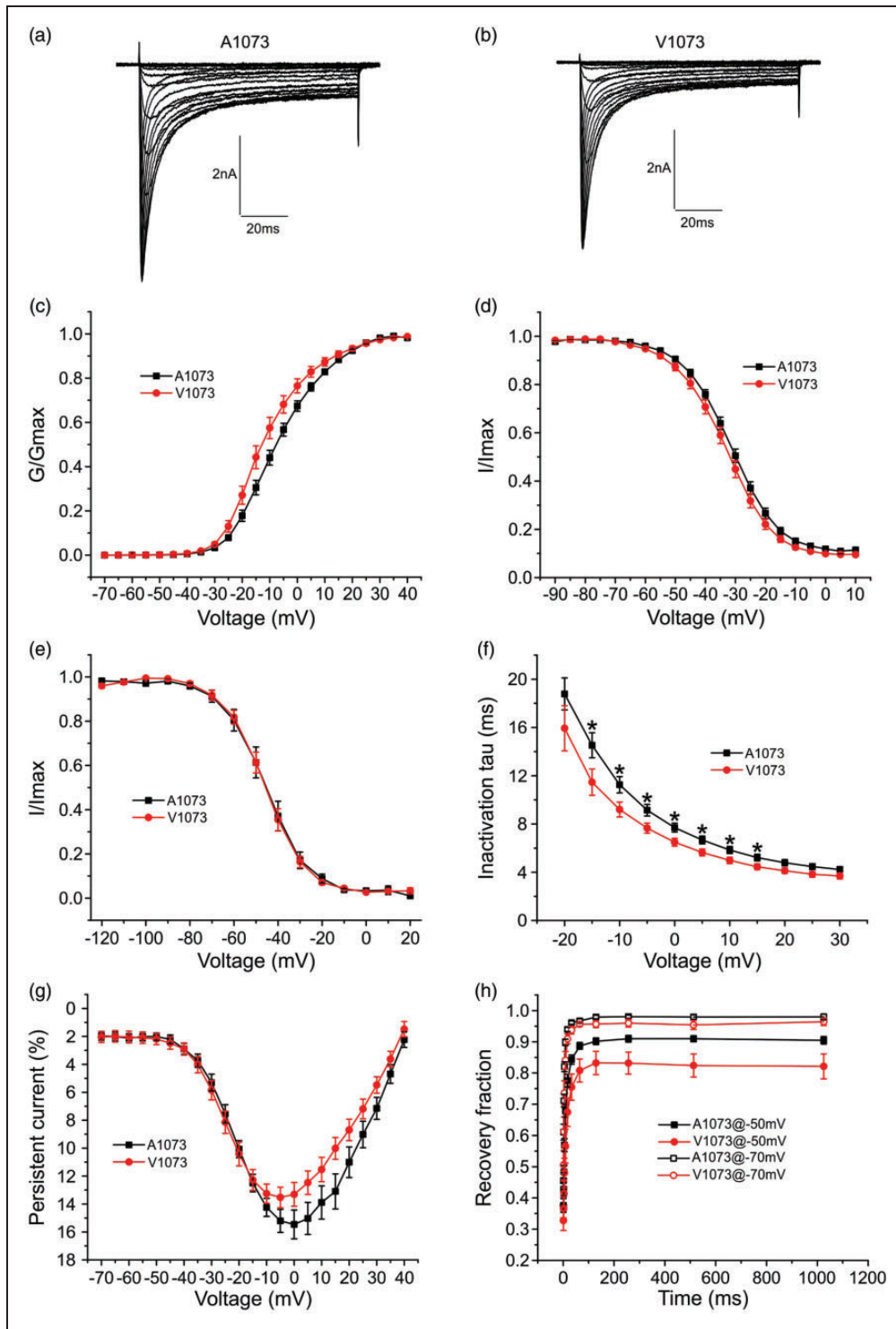


Figure 3. Voltage-clamp analysis of Nav1.8-Ala1073 and Nav1.8-Val1073 channels. (a and b) Representative Nav1.8 current family traces recorded from mouse Nav1.8-knockout DRG neurons transfected with Nav1.8-Ala1073 (a) or Nav1.8-Val1073 (b) channels. Cells were held at -70 mV and stepped to a range of potentials (-70 to $+40$ mV in 5-mV increments) for 100 ms. (c) Comparison of voltage-dependent activation between Nav1.8-Ala1073 and Nav1.8-Val1073 channels. Activation of Nav1.8-Val1073 channels is hyperpolarized by 4.3 mV compared with Nav1.8-Ala1073 channels. (d) Fast inactivation of Nav1.8-Val1073 channels is not significantly different from that of Nav1.8-Ala1073 channels. (e) Slow inactivation of Nav1.8-Val1073 channels is not significantly different from that of Nav1.8-Ala1073 channels. (f) Nav1.8-Val1073 channels display faster inactivation kinetics compared with Nav1.8-Ala1073 channels, $*P < 0.05$. (g) Comparison of persistent current between Nav1.8-Ala1073 channels and Nav1.8-Val1073 channels. (h) Comparison of recovery from fast inactivation between Nav1.8-Ala1073 and Nav1.8-Val1073 channels at -70 mV and -50 mV. Nav1.8-Val1073 channels tend to recovery more slowly from inactivation than Nav1.8-Ala1073 channels at both -70 mV and -50 mV.

between DRG neurons expressing Nav1.8-Ala1073 channels and DRG neurons expressing Nav1.8-Val1073 channels and found no significant difference (Nav1.8-Ala1073: -31.4 ± 1.0 mV, $n=29$; Nav1.8-Val1073: -29.6 ± 1.1 mV, $n=33$, $P > 0.05$). There was no significant difference for either action potential amplitude (Nav1.8-Ala1073: 113.0 ± 1.5 mV, $n=29$; Nav1.8-Val1073: 114.5 ± 1.6 mV, $n=33$, $P > 0.05$) or half-width of action potentials (Nav1.8-Ala1073: 10.6 ± 1.7 ms, $n=29$; Nav1.8-Val1073: 10.5 ± 0.8 ms, $n=33$, $P > 0.05$) between the two groups of DRG neurons.

The effect of Nav1.8-Ala1073 and Nav1.8-Val1073 channels on the repetitive firing properties of DRG neurons was assessed by applying a series of 500-ms current injections to the two groups of DRG neurons. Figure 4(a) shows the responses of representative DRG neurons expressing either Nav1.8-Ala1073 or Nav1.8-Val1073 channels to 500-ms current steps at 1X, 2X, and 3X current threshold. In contrast to the neuron expressing Nav1.8-Ala1073 channels, the neuron expressing Nav1.8-Val1073 channels generated fewer action potentials in response to the current injections at a range of different stimuli. Figure 4(b) displays a comparison of the average number of action potentials between these two groups of DRG neurons evoked by 500-ms current steps at a spectrum of stimulus strengths. DRG neurons transfected with Nav1.8-Val1073 channels fired at a significantly lower frequency than DRG neurons transfected with Nav1.8-Ala1073 ($P < 0.05$, Scheirer-Ray-Hare test).

In addition, we observed that among both groups of DRG neurons, a subpopulation of neurons fired spontaneously. The proportion of spontaneously firing neurons for the group of DRG neurons expressing Nav1.8-Val1073 channels (14 out of 47 cells, 29.8%) was lower than that of the group of DRG neurons expressing Nav1.8-Ala1073 channels (19 out of 48 cells, 39.6%), although this difference did not reach statistical significance ($P > 0.05$, two-portion z test). We also analyzed the membrane potential oscillation at the resting membrane potential between two groups of DRG neurons. For cells which did not display spontaneous firing, no obvious oscillations were observed in cells expressing Nav1.8-Ala1073 channels or Nav1.8-Val1073 channels. For spontaneously firing cells, a few cells from each group displayed comparable oscillations with low frequency (3~8Hz), but there is no significant difference between the two groups: Nav1.8-Val1073 channels, 3 out of 14 cells, 21.4%; Nav1.8-Ala1073 channels, 3 out of 19 cells, 15.8% ($P > 0.05$, two-portion z test). For evoked firing, the variability of the cellular responses to the stimulations precludes quantitative assessment of differences in oscillation properties between the two groups of neurons.

Discussion

It has been recently demonstrated that mutations in Nav1.8 sodium channels contribute to pain in a small percentage of cases of human peripheral neuropathy.⁹⁻¹¹ Here, we assessed the association of two common variants in *SCN10A* with pain in a discovery cohort and a relatively homogeneous replication population of female subjects of Chinese Han descent. We demonstrated that carriers of the minor allele at position 1073 (rs6795970, G > A; p.Ala1073Val) manifest reduced mechanical pain sensitivity. Using voltage-clamp recordings in DRG neurons, we demonstrated that the Nav1.8-Val1073 shifts the voltage-dependence of activation 4.3 mV in a hyperpolarizing direction and displays faster inactivation kinetics. Using current-clamp in DRG neurons, we showed that DRG neurons expressing Nav1.8-Val1073 channels produce fewer evoked action potentials in response to prolonged depolarized stimuli compared to those expressing the Nav1.8-Ala1073 channels. The results of this candidate SNP association study and of functional testing in DRG neurons support a role for the *SCN10A* rs6795970 SNP in biasing human pain sensitivity.

Our results showed significant association with pressure pain threshold and pressure pain tolerance for both *SCN10A* nonsynonymous SNPs, rs6795970 and rs12632942, in the original cohort, but only the rs6795970 SNP showed significant association with reduced mechanical pain sensitivity in our replication cohort. In the current study, the original cohort was comprised of 309 female and 187 male university students (ratio of females to males: 1.65:1), while the second cohort was comprised exclusively of 1005 females. Therefore, the replication cohort was more homogenous and powerful than the discovery cohort. All mechanical pain measurement values in the replication cohort were lower than those in the discovery cohort, possibly due to differences in demographic characteristics especially age, sex, health status, and different test environment (Table 1).⁴⁵⁻⁴⁷ Thus, the replication population could be considered independent from the primary study population. These considerations strengthen our conclusion that rs6795970 is associated with reduced mechanical pain sensitivity, while the possible contribution of rs12632942 to pain needs further investigation.

Several human Nav1.8 mutations have been identified in patients with painful peripheral neuropathy and have met criteria for potential pathogenicity by predictive algorithms and functional testing in DRG neurons, linking this channel to pain.⁹⁻¹¹ Although identification of these mutations may explain rare pain syndromes, a search for common variants in the general population which associate with pain sensitivity has not been previously reported. Data presented in this study show that a common polymorphism in the *SCN10A* gene is

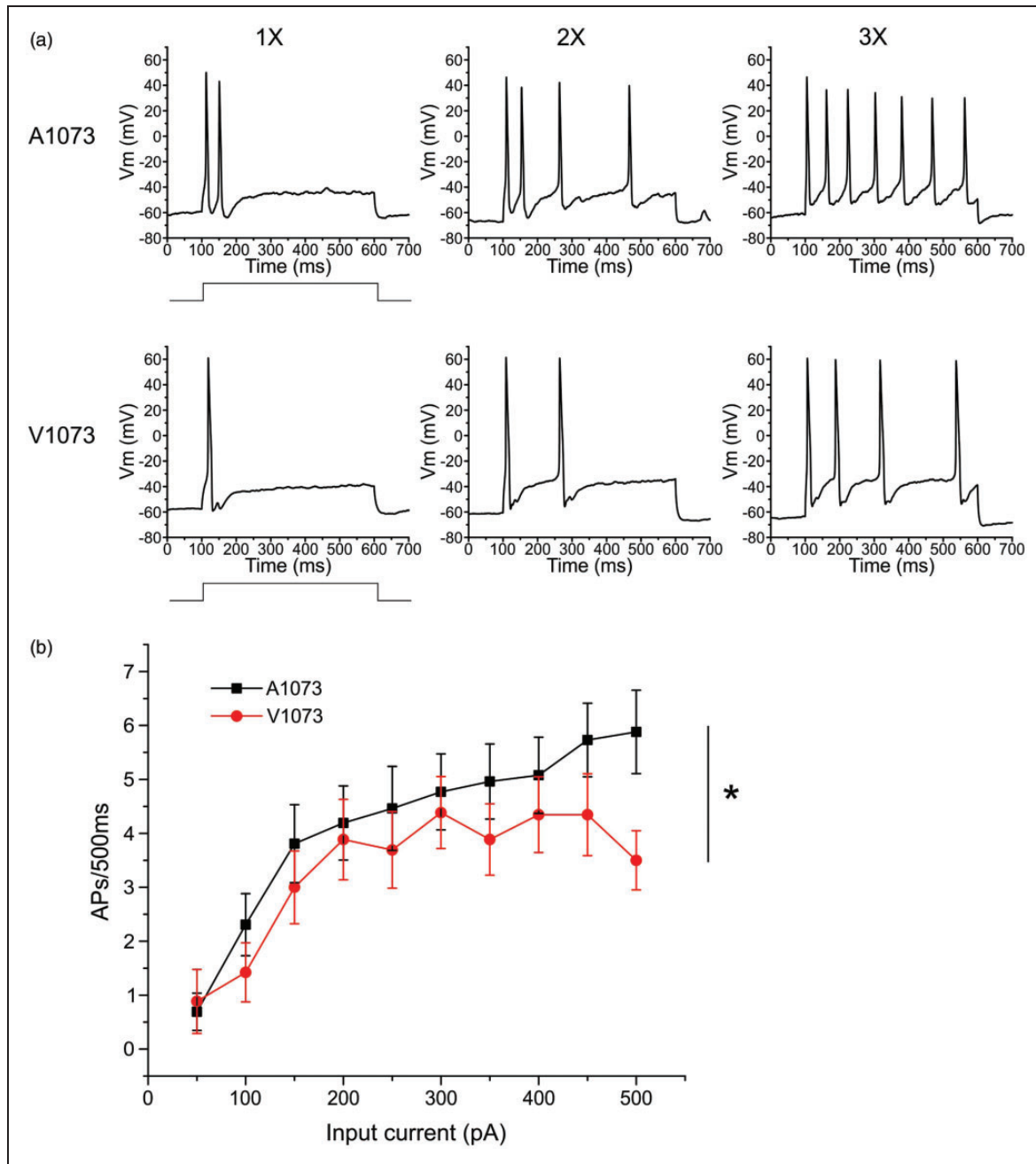


Figure 4. Compared with Nav1.8-Ala1073 channels, Nav1.8-Val1073 channels decrease firing frequency in small DRG neurons. (a) Response of cells expressing Nav1.8-Ala1073 and Nav1.8-Val1073 channels, respectively, to 500-ms depolarizing current steps that are 1X, 2X, and 3X (left, middle, and right traces, respectively) the current threshold for action potential generation. (b) Comparison of mean fire frequencies among cells expressing Nav1.8-Ala1073 and Nav1.8-Val1073 channels across the range of current injections from 50 to 500 pA, * $P < 0.05$, indicating statistical significance between two groups of neurons.

associated with mechanical pain sensitivity. Individuals carrying the homozygous minor allele (A/A) of rs6795970 in the replication cohort of 1005 female subjects showed an association with S-PPT which reached statistical significant after BONF correction when compared to carriers of the homozygous major alleles (G/G; $P = 2.4 \times 10^{-5}$) or heterozygous alleles (A/G;

$P = 2.3 \times 10^{-5}$); a significant difference in D-PPTs was also found between carriers of the A/A genotype and carriers of the homozygous major allele G/G (5.1×10^{-4}) or the heterozygous A/G alleles (7.2×10^{-4}). Together, our data support a role for Nav1.8 in regulating mechanical pain perception in humans.

Previously, rs6795970 was associated with slower cardiac conduction,^{12–21} but the direct functions of the Ala1073Val substitution on cardiac myocyte was unclear. Two previous studies explored effects of Ala1073Val by studying the gating properties of Nav1.8 in heterologous cell line expression systems.^{22,23} In these studies, Nav1.8 channels were expressed in ND7/23 cells²² or Neuro-2A cells.²³ By contrast, we conducted our functional assessments of Nav1.8/Ala1073Val in DRG neurons where this channel is normally expressed.¹ It is well established that different expression cell backgrounds may contribute to discordant results among the three studies. For example, both Behr et al.²² and Jabbari et al.²³ reported reduced current density for Val1073 compared to Ala1073 channels, while we did not detect a difference in the current density between the two channels in DRG neurons. For the steady-state fast inactivation, Behr et al.²² reported large hyperpolarization (−21.8 mV) for Val1073 channel compared with Ala1073 channel, but both Jabbari et al.²³ and our data did not show significant difference between the two channels. Behr et al.²² reported that the inactivation kinetics of Val1073 channel were slower than those of Ala1073 channel, which is at variance with Jabbari et al.²³ and our data. We present here the only functional assessment of Nav1.8/Ala1073Val at the cellular level, demonstrating a small but significant difference in evoked firing of DRG neurons. The relatively small size effect on DRG neuron firing is consistent with the pain phenotype, in particular with the reduced pain threshold of evoked pain in individuals, but without a pathological pain phenotype.

There are limitations to this study. Because we did not apply psychological tests in the replication sample, we cannot rule out a contribution of anxiety and/or depression to the outcome measures of experimental pain. It is worth noting that our current clamp data cannot completely reflect changes in pressure pain observed in human subjects carrying the different Nav1.8 alleles. In current clamp analysis, DRG neurons expressing Nav1.8-Val1073 channels produced fewer evoked action potentials in response to prolonged depolarized stimuli whereas it did not cause a significant effect on current threshold, compared to those expressing the Nav1.8-Ala1073 channels. Human subjects carrying the different alleles, however, manifested significant differences in both pressure pain threshold and pressure pain tolerance. The underlying mechanism for this discrepancy is not yet fully understood, and may reflect a limitation of extrapolating data from isolated neuronal cell bodies in culture to explain responses in human subjects.

In our voltage-clamp analysis, we observed that Val1073 accelerates the inactivation of Nav1.8 sodium channels, a loss-of-function attribute which may render DRG neuron hypoexcitable. However, Nav1.8-Val1073

also shifts the voltage dependence of activation 4.3 mV in a hyperpolarizing direction, a gain-of-function attribute which increases the excitability of DRG neurons. Although many sodium channel mutations which showed gain-of-function changes in voltage dependence of activation have been correlated with increased excitability of DRG neurons, Estacion et al.⁴⁸ reported that the sodium channel Nav1.7 variant Arg1150Trp which hyperpolarized voltage-dependent activation reduced the excitability of DRG neurons. More recently, Huang et al.⁴⁹ showed that expression of the Nav1.7 mutation Arg1279Pro which demonstrated mixed changes of biophysical properties of sodium channel Nav1.7, including depolarized voltage-dependent activation, increases the excitability of DRG neurons. Thus, a gain-of-function alteration of voltage-dependence of activation does not necessarily lead to increased excitability of DRG neurons if other properties are also changed. The net effect of a mutation with mixed biophysical properties must be empirically determined, as we have done in this study.

The Nav1.8 rs6795970SNP results in a coding change of Ala1073 by Val, which lies in the L2, intracellular loop between transmembrane domains II and III of the channel and the major effects of the Ala1073Val substitution are on gating properties of the Nav1.8 channel. Although the contribution of L2 to the gating mechanisms of the channel are not well understood, gain-of-function mutations in this region of Nav1.7, another peripheral sodium channel which plays a major role in regulating pain,⁵⁰ have been linked to painful small fiber neuropathy (Met932Leu/Val991Leu),⁵¹ and paroxysmal extreme pain disorder (Arg996Cys),⁵² and predispose carriers to neuropathic pain (Arg1150Trp).⁵³ The Ala1073Val substitution in Nav1.8 is functionally analogous to the Arg1150Trp substitution in Nav1.7 in that these two changes bias the pain phenotype rather than cause pathological pain as do the Nav1.7 mutations Arg996Cys and Met932Leu/Val991Leu.

Our previous results^{9–11} and data presented in this study support a role for *SCN10A* in regulating human pain sensitivity and in clinical pain conditions. Gain-of-function mutations in *SCN10A* produce pain in patients with peripheral neuropathy, and we now show that the SNP rs6795970 is associated with pain sensitivity in the general population. Lower pain sensitivity in our previous study, which included members of both discovery and replication cohorts, has also been associated with the *SCN9A* intronic SNP rs16851778,²⁷ for which there is no clear functional effect at this time. However, a limitation to our interpretation of the current results in the association study is that both discovery and replication cohorts were limited to a Chinese population. The minor homozygote frequency of rs6795970 A/A differs greatly in different racial groups, e.g., the frequency of A/A in the current population is 3.1%, while 1000G database (<http://>

www.1000genomes.org/) showed that it is 12.4 and 17.1 in American and European populations. Therefore, the association between rs6795970 and human pain sensitivity in other ethnic populations remains to be tested.

In summary, the D-PPT and S-PPT in subjects homozygous for the minor allele rs6795970 were 30% higher than in subjects with the other genotypes, with a highly significant BONF *P*-value reaching 2.3×10^{-5} . A contribution of rs6795970 in regulating excitability of DRG neurons was supported by our electrophysiology analysis. Taken together, our results support a role for Nav1.8 not only in pathological pain conditions but also in modulating human pain sensitivity in the general population. Demonstration of a role of this common variant in biasing pain sensitivity may facilitate the deep insight of the mechanism of interindividual differences in pain sensitivity and support targeting of this channel for treatment of pain.

Author Contribution

G. Duan: designed research, analyzed data and wrote manuscript; C. Han: collected and analyzed data, and wrote manuscript; Q. Wang, M. Zhang, and N. Li: collected blood sample; S. Guo, Y. Ying, P. Huang, and L. Zhang: performed pain tests; Y. Zhang: recruited subjects and collected data; L. Macala and P. Shah: provided critical reagents; S. D. Dib-Hajj: designed research, analyzed data, wrote and edited manuscript; S. G. Waxman: designed and supervised project, analyzed data, and wrote and edited manuscript; X. Zhang: designed and supervised project, analyzed data, and wrote and edited manuscript.

Declaration of Conflicting Interests

The author(s) declared no potential conflicts of interest with respect to the research, authorship, and/or publication of this article.

Funding

The author(s) disclosed receipt of the following financial support for the research, authorship, and/or publication of this article: This work was supported in part by grants to XZ from National Nature Science Foundation of China (81271235) and the Rehabilitation Research Service and Medical Research Service, Department of Veterans Affairs (SDH and SGW). The Center for Neuroscience & Regeneration Research is a Collaboration of the Paralyzed Veterans of America with Yale University.

References

1. Akopian AN, Sivilotti L and Wood JN. A tetrodotoxin-resistant voltage-gated sodium channel expressed by sensory neurons. *Nature* 1996; 379: 257–262.
2. Black JA and Waxman SG. Molecular identities of two tetrodotoxin-resistant sodium channels in corneal axons. *Exp Eye Res* 2002; 75: 193–199.
3. Persson AK, Black JA, Gasser A, et al. Sodium-calcium exchanger and multiple sodium channel isoforms in intra-epidermal nerve terminals. *Mol Pain* 2010; 6: 84.
4. Sangameswaran L, Fish LM, Koch BD, et al. A novel tetrodotoxin-sensitive, voltage-gated sodium channel expressed in rat and human dorsal root ganglia. *J Biol Chem* 1997; 272: 14805–14809.
5. Bennett DL and Woods CG. Painful and painless channelopathies. *Lancet Neurol* 2014; 13: 587–599.
6. Dib-Hajj SD, Cummins TR, Black JA, et al. Sodium channels in normal and pathological pain. *Annu Rev Neurosci* 2010; 33: 325–347.
7. Garrison SR, Weyer AD, Barabas ME, et al. A gain-of-function voltage-gated sodium channel 1.8 mutation drives intense hyperexcitability of A- and C-fiber neurons. *Pain* 2014; 155: 896–905.
8. Renganathan M, Cummins TR and Waxman SG. Contribution of Na(v)1.8 sodium channels to action potential electrogenesis in DRG neurons. *J Neurophysiol* 2001; 86: 629–640.
9. Faber CG, Lauria G, Merkies IS, et al. Gain-of-function Nav1.8 mutations in painful neuropathy. *Proc Natl Acad Sci USA* 2012; 109: 19444–19449.
10. Han C, Vasylyev D, Macala LJ, et al. The G1662S Nav1.8 mutation in small fibre neuropathy: impaired inactivation underlying DRG neuron hyperexcitability. *J Neurol Neurosurg Psychiatry* 2014; 85: 499–505.
11. Huang J, Yang Y, Zhao P, et al. Small-fiber neuropathy Nav1.8 mutation shifts activation to hyperpolarized potentials and increases excitability of dorsal root ganglion neurons. *J Neurosci* 2013; 33: 14087–14097.
12. Bezzina CR, Barc J, Mizusawa Y, et al. Common variants at SCN5A-SCN10A and HEY2 are associated with Brugada syndrome, a rare disease with high risk of sudden cardiac death. *Nat Genet* 2013; 45: 1044–1049.
13. Chambers JC, Zhao J, Terracciano CM, et al. Genetic variation in SCN10A influences cardiac conduction. *Nat Genet* 2010; 42: 149–152.
14. Denny JC, Ritchie MD, Crawford DC, et al. Identification of genomic predictors of atrioventricular conduction: using electronic medical records as a tool for genome science. *Circulation* 2010; 122: 2016–2021.
15. Holm H, Gudbjartsson DF, Arnar DO, et al. Several common variants modulate heart rate, PR interval and QRS duration. *Nat Genet* 2010; 42: 117–122.
16. Jeff JM, Ritchie MD, Denny JC, et al. Generalization of variants identified by genome-wide association studies for electrocardiographic traits in African Americans. *Ann Hum Genet* 2013; 77: 321–332.
17. Pfeufer A, van Noord C, Marcianti KD, et al. Genome-wide association study of PR interval. *Nat Genet* 2010; 42: 153–159.
18. Ritchie MD, Denny JC, Zuvich RL, et al. Genome- and phenome-wide analyses of cardiac conduction identifies markers of arrhythmia risk. *Circulation* 2013; 127: 1377–1385.

19. Sano M, Kamitsuji S, Kamatani N, et al. Genome-wide association study of electrocardiographic parameters identifies a new association for PR interval and confirms previously reported associations. *Hum Mol Genet* 2014; 23: 6668–6676.
20. Smith JG, Magnani JW, Palmer C, et al. Genome-wide association studies of the PR interval in African Americans. *PLoS Genet* 2011; 7: e1001304.
21. Sotoodehnia N, Isaacs A, de Bakker PI, et al. Common variants in 22 loci are associated with QRS duration and cardiac ventricular conduction. *Nat Genet* 2010; 42: 1068–1076.
22. Behr ER, Savio-Galimberti E, Barc J, et al. Role of common and rare variants in SCN10A: results from the Brugada syndrome QRS locus gene discovery collaborative study. *Cardiovasc Res* 2015; 106: 520–529.
23. Jabbari J, Olesen MS, Yuan L, et al. Common and rare variants in SCN10A modulate the risk of atrial fibrillation. *Circ Cardiovasc Genet* 2015; 8: 64–73.
24. Delaney JT, Muhammad R, Shi Y, et al. Common SCN10A variants modulate PR interval and heart rate response during atrial fibrillation. *Europace* 2014; 16: 485–490.
25. Verkerk AO, Remme CA, Schumacher CA, et al. Functional Nav1.8 channels in intracardiac neurons: the link between SCN10A and cardiac electrophysiology. *Circ Res* 2012; 111: 333–343.
26. Yang T, Atack TC, Stroud DM, et al. Blocking Scn10a channels in heart reduces late sodium current and is anti-arrhythmic. *Circ Res* 2012; 111: 322–332.
27. Duan G, Guo S, Zhang Y, et al. The effect of SCN9A variation on basal pain sensitivity in the general population: an experimental study in young women. *J Pain* 2015; 16: 971–980.
28. Pauli P, Wiedemann G and Nickola M. Pressure pain thresholds asymmetry in left- and right-handers: associations with behavioural measures of cerebral laterality. *Eur J Pain* 1999; 3: 151–156.
29. Chanock SJ, Manolio T, Boehnke M, et al. Replicating genotype-phenotype associations. *Nature* 2007; 447: 655–660.
30. Tian C, Gregersen PK and Seldin MF. Accounting for ancestry: population substructure and genome-wide association studies. *Hum Mol Genet* 2008; 17: R143–150.
31. Duan G, Guo S, Zhan H, et al. A new real-time method for detecting the effect of fentanyl using the preoperative pressure pain threshold and Narcotrend index: a randomized study in female surgery patients. *Medicine (Baltimore)* 2015; 94: e316.
32. Guo S, Duan G, Wang J, et al. Comparison of sufentanil-tramadol PCIA between laparoscopic cholecystectomy and gynecological laparoscopy. *Zhong hua Wai Ke Za Zhi* 2015; 53: 150–154.
33. Fillingim RB, King CD, Ribeiro-Dasilva MC, et al. Sex, gender, and pain: a review of recent clinical and experimental findings. *J Pain* 2009; 10: 447–485.
34. Duan G, Xiang G, Zhang X, et al. An improvement of mechanical pain sensitivity measurement method: the smaller sized probes may detect heterogeneous sensory threshold in healthy male subjects. *Pain Med* 2014; 15: 272–280.
35. Duan G, Xiang G, Zhang X, et al. A single-nucleotide polymorphism in SCN9A may decrease postoperative pain sensitivity in the general population. *Anesthesiology* 2013; 118: 436–442.
36. Montagne-Clavel J and Oliveras JL. The “plantar test” apparatus (Ugo Basile Biological Apparatus), a controlled infrared noxious radiant heat stimulus for precise withdrawal latency measurement in the rat, as a tool for humans? *Somatosens Mot Res* 1996; 13: 215–223.
37. Sinville R, Coyne J, Meagher RJ, et al. Ligase detection reaction for the analysis of point mutations using free-solution conjugate electrophoresis in a polymer microfluidic device. *Electrophoresis* 2008; 29: 4751–4760.
38. Atkins JF, Wills NM, Loughran G, et al. A case for “StopGo”: reprogramming translation to augment codon meaning of GGN by promoting unconventional termination (Stop) after addition of glycine and then allowing continued translation (Go). *RNA* 2007; 13: 803–810.
39. Luke GA, de Felipe P, Lukashev A, et al. Occurrence, function and evolutionary origins of ‘2A-like’ sequences in virus genomes. *J Gen Virol* 2008; 89: 1036–1042.
40. Ryan MD and Drew J. Foot-and-mouth disease virus 2A oligopeptide mediated cleavage of an artificial polyprotein. *EMBO J* 1994; 13: 928–933.
41. Dib-Hajj SD, Choi JS, Macala LJ, et al. Transfection of rat or mouse neurons by biolistics or electroporation. *Nat Protoc* 2009; 4: 1118–1126.
42. Stirling LC, Forlani G, Baker MD, et al. Nociceptor-specific gene deletion using heterozygous Nav1.8-Cre recombinase mice. *Pain* 2005; 113: 27–36.
43. Amir R, Michaelis M and Devor M. Membrane potential oscillations in dorsal root ganglion neurons: role in normal electrogenesis and neuropathic pain. *J Neurosci* 1999; 19: 8589–8596.
44. Amir R, Michaelis M and Devor M. Burst discharge in primary sensory neurons: triggered by subthreshold oscillations, maintained by depolarizing afterpotentials. *J Neurosci* 2002; 22: 1187–1198.
45. Castillo RC, Wegener ST, Heins SE, et al. Longitudinal relationships between anxiety, depression, and pain: results from a two-year cohort study of lower extremity trauma patients. *Pain* 2013; 154: 2860–2866.
46. Kroenke K, Wu J, Bair MJ, et al. Reciprocal relationship between pain and depression: a 12-month longitudinal analysis in primary care. *J Pain* 2011; 12: 964–973.
47. Riley JL 3rd, Cruz-Almeida Y, Glover TL, et al. Age and race effects on pain sensitivity and modulation among middle-aged and older adults. *J Pain* 2014; 15: 272–282.
48. Estacion M, Harty TP, Choi JS, et al. A sodium channel gene SCN9A polymorphism that increases nociceptor excitability. *Ann Neurol* 2009; 66: 862–866.
49. Huang J, Yang Y, Dib-Hajj SD, et al. Depolarized inactivation overcomes impaired activation to produce DRG neuron hyperexcitability in a Nav1.7 mutation in a patient with distal limb pain. *J Neurosci* 2014; 34: 12328–12340.

50. Dib-Hajj SD, Yang Y, Black JA, et al. The Na(V)1.7 sodium channel: from molecule to man. *Nat Rev Neurosci* 2013; 14: 49–62.
51. Faber CG, Hoeijmakers JG, Ahn HS, et al. Gain of function Nav1.7 mutations in idiopathic small fiber neuropathy. *Ann Neurol* 2012; 71: 26–39.
52. Fertleman CR, Baker MD, Parker KA, et al. SCN9A mutations in paroxysmal extreme pain disorder: allelic variants underlie distinct channel defects and phenotypes. *Neuron* 2006; 52: 767–774.
53. Reimann F, Cox JJ, Belfer I, et al. Pain perception is altered by a nucleotide polymorphism in SCN9A. *Proc Natl Acad Sci U S A* 2010; 107: 5148–5153.